View metadata, citation and similar papers at core.ac.uk
brought to you by CORE
provided by DSpace at VU

Journal of Mechanics in Medicine and Biology
Vol. 13, No. 1 (2013) 1350009 (18 pages)
© World Scientific Publishing Company
DOI: 10.1142/S0219519413500097

World Scientific
www.worldscientific.com

RELATIVE CONTRIBUTION OF DIFFERENT MUSCLE ENERGY CONSUMPTION PROCESSES IN AN ENERGY-BASED MUSCLE LOAD SHARING COST FUNCTION

ALI A. NIKOOYAN[*,§], HEJ VEEGER[*,†], PETER WESTERHOFF[‡], GEORG BERGMANN[‡] and FRANS C. T. VAN DER HELM[*]

[*]*Department of Biomechanical Engineering*
Delft University of Technology
Mekelweg 2, Delft 2628CD, The Netherlands

[†]*Research Institute Move, VU Amsterdam*
Van der Boechorststraat 9
1081BT Amsterdam, The Netherlands

[‡]*Julius Wolff Institut, Charité, Universitätsmedizin*
Augustenburger Platz 1, 13353 Berlin, Germany
[§]*a.asadinikooyan@tudelft.nl*
[§]*aanikooyan@gmail.com*

Received 31 October 2011
Revised 26 June 2012
Accepted 2 July 2012
Published 10 August 2012

The aim of this study is to quantify the relative contributions of two muscle energy consumption processes (the detachment of cross-bridges and calcium-pumping) incorporated in a recently developed muscle load sharing cost function, namely the energy-based criterion, by using *in vivo* measured glenohumeral-joint reaction forces (GH-JRFs). Motion data and *in vivo* GH-JRFs were recorded for four patients carrying an instrumented shoulder implant while performing abduction and forward flexion motions up to their maximum possible arm elevations. Motion data were used as the input to the delft shoulder and elbow model for the estimation of GH-JRFs. The widely used stress as well as the energy-based cost functions were adopted as the load sharing criteria. For the energy-based criterion, simulations were run for a wide range of different weight parameters (determining the relative contribution of the two energy processes) in the neighborhood of the previously assumed parameters for each subject and motion. The model-predicted and *in vivo*-measured GH-JRFs were compared for all model simulations. Application of the energy-based criterion with new identified parameters resulted in significant (two-tailed $p < 0.05$, post-hoc power ~ 0.3) improvement (on average $\sim$20%) of the model-predicted GH-JRFs at the maximal arm elevation compared to when using either the stress or the pre-assumed form of the energy-based criterion. About 25% of the total energy consumption was calculated for the calcium-pumping process at maximal muscle activation level when using the new parameters. This value was comparable to the corresponding ones reported in the

[§]Corresponding author.

J. Mech. Med. Biol. 2013.13. Downloaded from www.worldscientific.com
by VU UNIVERSITY AMSTERDAM LIBRARY on 03/25/13. For personal use only.

previous literature. The identified parameters are recommended to be used instead of their predecessors.

Keywords: Shoulder; glenohumeral joint; musculoskeletal model; inverse dynamics; cross-bridges cycling; calcium pumping.

J. Mech. Med. Biol. 2013.13. Downloaded from www.worldscientific.com
by VU UNIVERSITY AMSTERDAM LIBRARY on 03/25/13. For personal use only.

1. Introduction

Detailed information about muscle function and forces in the human musculoskeletal system is demanded for several applications such as improvement of the design and preclinical testing of endoprostheses or design of the treatments of motor disorders. Nevertheless, measuring the muscle forces *in vivo* is hardly possible by non-invasive methods. This explains why biomechanical models of the neuromusculoskeletal system have been invented to estimate muscle forces based on external measurements. To date, biomechanical models are still the only means of estimation of muscle forces, certainly outside laboratory conditions. In the last few decades, a variety of models of the entire human musculoskeletal system from simple two-dimensional[1–3] to complex three-dimensional models,[4–6] have been developed.

Inverse dynamics and forward dynamics modeling are two major approaches for the estimation of internal loads within the musculoskeletal system. Although inverse dynamics optimization is noticeably faster than forward optimization, it faces an indeterminacy problem for the calculation of individual muscle forces from net joint moment. More than one combination of muscle forces may produce the same given net moment around a joint. It is not yet understood how the central nervous system shares the loads among all muscles passing a joint. We attempted to approximate the load sharing of the human by minimizing a "cost function" to find a relatively arbitrary "optimal" solution.

Several cost functions have been introduced,[7] among which two are being used in this study. The first criterion, the quadratic stress cost function (SCF),[8] is the most widely used criterion in the inverse dynamics-based musculoskeletal models and minimizes the summed muscle stress around a joint. The second criterion is called the energy-based cost function (ECF).[9] This criterion is based on two main energy consuming processes in a muscle needed to produce a contraction, namely detachment of cross bridges and re-uptake of calcium.[10] Both cost functions have been implemented and used in a comprehensive musculoskeletal model of the shoulder and elbow, the delft shoulder and elbow model (DSEM),[11] which is the core model in this study.

In a previous study,[10] the SCF and ECF were compared based on the muscle oxygen consumption using near infrared spectroscopy, where the ECF was favored due to its better qualitative consistency with the measured oxygen consumption, specifically for the elbow muscles. Later,[12] it was shown that in comparison with the SCF, the ECF results in better consistency between experimental results and the DSEM predicted principal actions. In a recent study,[13] the glenohumeral-joint reaction forces (GH-JRFs) estimated by the DSEM were compared to those measured

in vivo using an instrumented shoulder implant.[14] Both SCF and ECF were used in the inverse optimization process to calculate the GH-JRFs. The results showed that the model generally underestimated the GH-JRFs for dynamic tasks like abduction (Abd) and forward flexion (FF), but also that model estimations using the two cost functions differed up to 8%.

There is no agreement either for techniques or results among various studies that attempted to quantify the relative contributions of different energy consumption processes for single muscles. *In vitro* measurements were carried out for maximal[15–21] or submaximal[22–26] isometric single fiber muscle contractions. As for maximal isometric contractions, one may conclude from the literature that about 23−44% of the total energy consumption is related to the ion (Ca^{2+} and/or Na^{+}) pumping and the remainder is related to cross-bridges cycling. In a review study, Barclay *et al.*[27] concluded that regardless of muscle contractile properties, the techniques used for measuring the energy consumption, and experimental conditions, the contribution of Ca^{2+} pumping is more or less the same ($\sim$30−40% of the total energy consumption) for muscles from mammals in isometric contraction. In the study by Praagman *et al.*,[10] the relative contribution of the two processes in the ECF was unknown and the two terms were implemented based on the assumption of a 1:1 (cross-bridges to calcium pumping) contribution at 50% activation during an isometric contraction.

In this study, we aim to estimate a separate contribution of the two energy consumption processes in the ECF which

(1) coincides with the corresponding values in the literature, and
(2) can lead to a closer match between the model (i.e., the DSEM) and the experiment as for the GH-JRFs.

To this end, the kinematic data from four patients with an instrumented shoulder endoprosthesis were used as model input. The inverse dynamic simulation was performed using the model (DSEM) and by recruiting both cost functions (SCF and ECF) as the muscle load sharing criteria. For the ECF, the simulation process was repeated for a variety of different adjusting parameters of the ECF. All model-simulated GH-JRFs were compared to those measured *in vivo* to identify new parameter sets. The new identified parameter sets were then applied to calculate the relative contribution of the two energy terms and the results compared to the corresponding values in the literature. It was expected that by using the new identified weight parameters of the ECF, more realistic model predictions of the glenohumeral joint reaction forces can be obtained.

2. Methodology

2.1. *Inverse dynamic musculoskeletal model*

The DSEM is a comprehensive three-dimensional model of human shoulder and elbow.[11,28] The geometrical data for the model were obtained through detailed

J. Mech. Med. Biol. 2013.13. Downloaded from www.worldscientific.com
by VU UNIVERSITY AMSTERDAM LIBRARY on 03/25/13. For personal use only.

J. Mech. Med. Biol. 2013.13. Downloaded from www.worldscientific.com
by VU UNIVERSITY AMSTERDAM LIBRARY on 03/25/13. For personal use only.

cadaver studies.[29] The model is basically inverse dynamics-based, although it offers forward dynamics and combined inverse-forward dynamics options as well. The recorded motions of the bony segments (i.e., joint angles) and external loads are used as input to the model and muscle and joint reaction forces are calculated as model outputs through an inverse dynamics analysis.

2.2. *The energy-based muscle load sharing cost function*

The energy-based muscle load sharing criterion is based on two main energy consuming processes in a muscle needed to produce a contraction, namely detachment of cross bridges and re-uptake of calcium. This cost function (J_E) was originally introduced by Praagman *et al.*[10] for isometric contraction as follows:

$$J_E = \sum_{i=1}^{n} \{\dot{E}_{cb_i} + \dot{E}_{ca_i}\} = \sum_{i=1}^{n} \left\{ m_i \cdot \left(c_1 \frac{F_i}{PCSA_i} + c_2 \cdot \left(\frac{F_i}{PCSA_i \cdot \sigma_{\max}} \right)^2 \right) \right\}, \quad (1)$$

where i stands for the muscle element and n is the total number of muscle elements. $\dot{E}_{cb}$ and $\dot{E}_{ca}$ represent the two energy consumption processes including the detachment of cross-bridges and calcium pumping, respectively. F is the muscle force (N), m is the muscle mass (gr), $PCSA$ is the muscle physiological cross sectional area (cm^2), and $\sigma_{\max}$ is defined as $100\,\mathrm{N/cm}^2$.[30] c_1 and c_2 are constants indicating the relative contribution of the two energy terms.

The relative contribution of the two processes ($\dot{E}_{cb}$ and $\dot{E}_{ca}$) was unknown, and the two terms were implemented based on the assumption of a 1:1 (cross-bridges to calcium pumping) contribution at 50% activation during an isometric contraction.[10] This assumption resulted in 1:2 ratio at 100% activation.

Following a detailed cadaver study on the shoulder,[29] information about muscle architecture and optimal fiber length (l_{opt}) was obtained, which made it possible to implement the muscle dynamics in the inverse optimization process. The original form of the energy-based cost function was therefore, reformulated in order to take the muscle force-length relationship into account[9] as follows:

$$\begin{aligned} J_E &= \sum_{i=1}^{n} \{\dot{E}_{cb_i} + \dot{E}_{ca_i}\} \\ &= \sum_{i=1}^{n} \left\{ F_i \cdot l_{opt_i} + wf_1 \cdot m_i \cdot \left(\frac{F_i}{F_{i\max}(l)} + wf_2 \cdot \left(\frac{F_i}{F_{i\max}(l)} \right)^2 \right) \right\}, \end{aligned} \quad (2)$$

where l_{opt} is the optimal muscle fiber length (cm).

$F_{\max}(l)$ is the maximum muscle force (N) and is calculated as follows:

$$F_{\max}(l) = f(l_s) \cdot PCSA \cdot \sigma_{\max}, \quad (3)$$

where $f(l_s)$ is the normalized muscle force-length relationship.[31]

wf_1 and wf_2 are adjustable weight factors. wf_1 is an indication of the relative contribution of the two energy terms. wf_2 determines the shares of the linear and nonlinear parts in $\dot{E}_{ca}$, but also indirectly affects the relative contribution of the two

energy terms. Due to the lack of existing physiological knowledge, the weight parameters wf_1 and wf_2 were arbitrarily set as 100 and 4, respectively.[9]

2.3. *Data recordings*

Four patients (Table 1) carrying an instrumented shoulder hemi-arthroplasty[14] were used as subjects, and the data were recorded. Joint replacement was based on the diagnosis of progressed osteoarthritis without serious rotator cuff damage. The surgical approach was deltopectoral during which no nerve was damaged. The ethical committee of the FreieUniversität and Charité-Universitätsmedizin Berlin gave permission for the clinical studies where the instrumented endoprosthesis was used. Before, surgery patients were informed about the aims and procedures of all measurements after which they agreed to participate and signed an informed consent.

Measurements comprised the collection of motion data needed for model input, as well as *in vivo* GH-JRFs. For motion recordings, marker clusters on bony segments, including the thorax, scapula, upper arm, and forearm, were measured using four Optotrak (Northern Digital Inc., Canada, accuracy to 0.3 mm) camera bars at a sampling frequency of 50 Hz. In the calibration process, the spatial positions of anatomical landmarks on bony segments (Table 2) were recorded relative to technical marker clusters on those segments. The anatomical landmark selection was based on the ISB standardization protocol for upper extremity.[32] The glenohumeral joint rotation center, which was necessary for the reconstruction of the local coordinate system of the humerus, but could not be palpated *in vivo*, was estimated using the instantaneous helical axes (IHA) method.[33] Measured tasks comprised standard dynamic motions including Abd and FF up to maximum possible arm elevation. For scapular motion tracking, an acromion sensor[34] was used.

To measure the forces in the glenohumeral joint *in vivo*, a BIOMET Biomodular shoulder hemi-prosthesis was equipped with six strain gages, a nine-channel telemetry, and a coil for inductive power supply.[14] The *in vivo* measured contact forces were transferred to the external measuring equipment, and were then synchronized and resampled with the motion recording frequency (i.e., 50 Hz) to allow for further processing. For synchronization, the trigger signal from the Optotrak system was used.

2.4. *Modeling simulations*

Calculated joint angles from measured marker data were used as DSEM inputs. Model simulations were performed for Abd and FF motions and for four measured

Table 1. Detailed information of the measured subjects.

Subject	Sex	Age	Weight (kg)	Height (cm)	Implant side
S1	Female	73	72	168	Left
S2	Male	64	85	163	Right
S3	Male	69	93	173	Right
S4	Male	74	83	173	Right

J. Mech. Med. Biol. 2013.13. Downloaded from www.worldscientific.com
by VU UNIVERSITY AMSTERDAM LIBRARY on 03/25/13. For personal use only.

Table 2. The palpated anatomical landmarks in the calibration process.

Bony segment	Palpated landmark	Abbreviation
Thorax	Incisura Jugularis	IJ
	Processus Xiphoideus	PX
	Processus Spinosus of the 7th cervical vertebra	C7
	Processus Spinosus of the 8th thoracic vertebra	T8
Clavicle	Most ventral point on the sternoclavicular joint	SC
	Most dorsal point on the acromioclavicular joint	AC
Scapula	Angulus Acromialis	AA
	Trigonum Spinae	TS
	Angulus Inferior	AI
	Most ventral point of processus coracoideus	PC
Humerus (upper arm)	Most caudal point on medial epicondyle	EM
	Most caudal point on lateral epicondyle	EL
Forearm	Most caudal−lateral point on the radial styloid	SR
	Most caudal−medial point on the ulnar styloid	SU

J. Mech. Med. Biol. 2013.13. Downloaded from www.worldscientific.com
by VU UNIVERSITY AMSTERDAM LIBRARY on 03/25/13. For personal use only.

subjects. Both SCF and ECF served as the muscle load sharing criteria for inverse optimization. When ECF was used for optimization, each task and subject simulations were repeated for different combinations of weight factors [wf_1 and wf_2, Eq. (1)] in the ECF. The weight factors were changed in large ranges in the neighborhood of the default values (i.e. $wf_1 = 100$, $wf_2 = 4$, see Section 2.2) as follows:

$$\begin{cases} 1 \le wf_1 \le 200, & \text{step size} = 10 \\ 0 \le wf_2 \le 20, & \text{step size} = 1, \quad \text{and} \quad wf_2 = 100. \end{cases} \tag{4}$$

$wf_2 = 100$ was selected to study the effects of using a very high share of the nonlinear term in the $\dot{E}_{ca}$ on the modeling outcomes. The selected ranges led to 638 series of simulations for each motion and each subject. The muscle forces and GH-JRFs were calculated as outputs of the inverse dynamics analysis.

2.5. *Measure of goodness-of-fit*

For the evaluation of results, the model-calculated and *in vivo*-measured GH-JRFs were compared for all sets of simulations. To measure the goodness-of-fit, we used two indicators including (1) the root mean squared error (RMSE) between the model-estimated and measured GH-JRFs at all points, and (2) the error calculated at the maximal arm elevation angle ($\alpha_{\max}$) defined as the difference between estimated and measured GH-JRFs normalized to the measured force ($E_{\alpha\max}$). For $E_{\alpha\max}$, a negative value means an underestimation of the model with respect to the measured one, while a positive value indicates an overestimation.

For each subject and each motion, the contour graphs for RMSE and $E_{\alpha\max}$ were plotted for different values of the weight factors (Figs. 1 and 2). To ensure color consistency between the subplots, the positive values of $E_{\alpha\max}$ ($|E_{\alpha\max}|$) are plotted. Therefore, one should note that all values of $E_{\alpha\max}$ in Figs. 1 and 2 must be read as negative.

J. Mech. Med. Biol. 2013.13. Downloaded from www.worldscientific.com
by VU UNIVERSITY AMSTERDAM LIBRARY on 03/25/13. For personal use only.

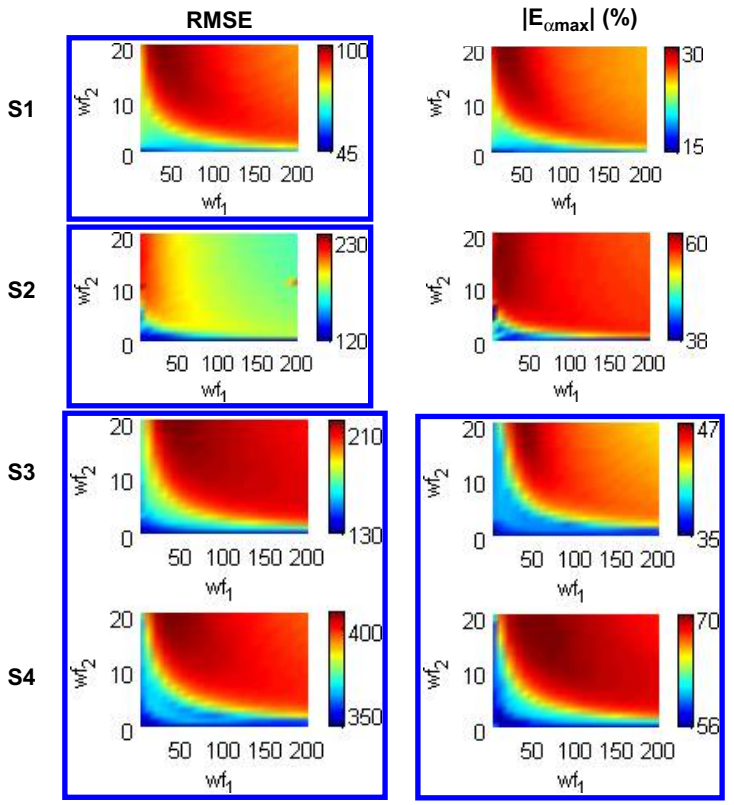

Fig. 1. The root mean squared error (RMSE) and absolute error at maximal arm elevation ($|E_{\alpha\max}|$) calculated between model-estimated and *in vivo*-measured GH-JRFs at different combinations of the weight factors (wf_1 and wf_2) of the ECF and for the four measured subjects during performing Abd motion.

The combination of wf_1 and wf_2 that resulted in the minimum value of RMSE was selected as the best solution (ECF_{best}). Except for one case (i.e., S2 during FF, Table 3), the best results were acquired when $1 \leq wf_1, wf_2 \leq 10$ (Table 3). Based on these results, three sets of weight factors were selected for more detailed follow-up comparisons as follows:

(1) The mean of the values presented in Table 3, i.e., $wf_1 = 4$, $wf_2 = 5$ (ECF_{mean}), and
(2) The two extreme parameter sets, i.e., $wf_1 = 1$, $wf_2 = 10$ ($\text{ECF}_{1,10}$) and $wf_1 = 10$, $wf_2 = 1$ ($\text{ECF}_{10,1}$).

The RMSE and $E_{\alpha\max}$ were calculated when using the three above-mentioned combinations of weight factors for the ECF as well as the default form of the ECF ($wf_1 = 100$, $wf_2 = 4$, ECF_{def}), and the SCF during both Abd and FF and for all subjects (Fig. 3).

J. Mech. Med. Biol. 2013.13. Downloaded from www.worldscientific.com
by VU UNIVERSITY AMSTERDAM LIBRARY on 03/25/13. For personal use only.

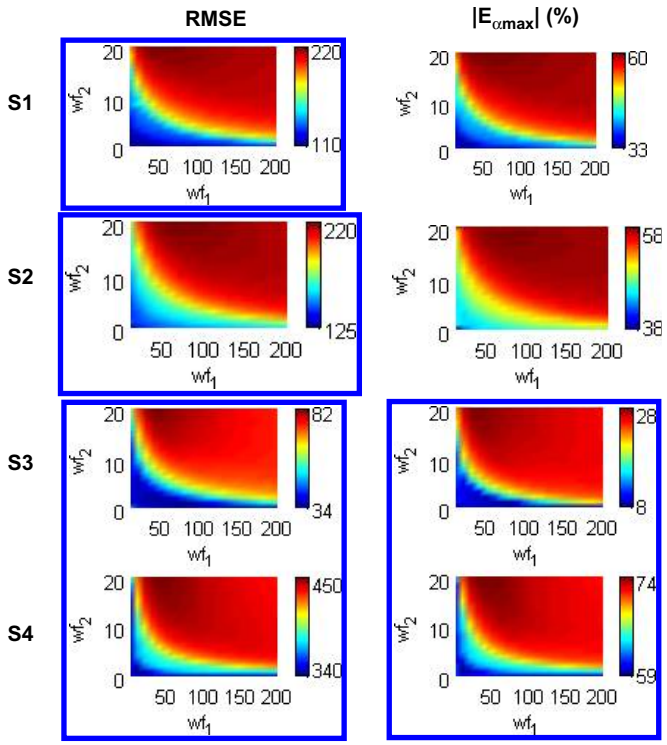

Fig. 2. The root mean squared error (RMSE) and absolute error at maximal arm elevation ($|E_{\alpha\,\max}|$) calculated between model-estimated and *in vivo* measured GH-JRFs at different combinations of the weight factors (wf_1 and wf_2) of the ECF and for the four measured subjects during performing FF motion.

Table 3. The combinations of wf_1 and wf_2 that resulted in the minimum value of RMSE between the model-estimated and measured GH-JRFs (the best solution) for different subjects and motions.

	Abd				FF				
	S1	S2	S3	S4	S1	S2	S3	S4	Mean
wf_1	3	3	1	1	1	9	10	1	4
wf_2	2	1	1	6	3	19	1	9	5

2.6. *Statistical analysis*

For statistical analysis, a two-tailed paired Students' *t*-test was used. The threshold for statistical significance was considered as 0.05. Post-hoc statistical power analysis for two-tailed Student's *t*-test was also carried out in order to evaluate the power of test with low number of subjects ($n = 4$).

J. Mech. Med. Biol. 2013.13. Downloaded from www.worldscientific.com
by VU UNIVERSITY AMSTERDAM LIBRARY on 03/25/13. For personal use only.

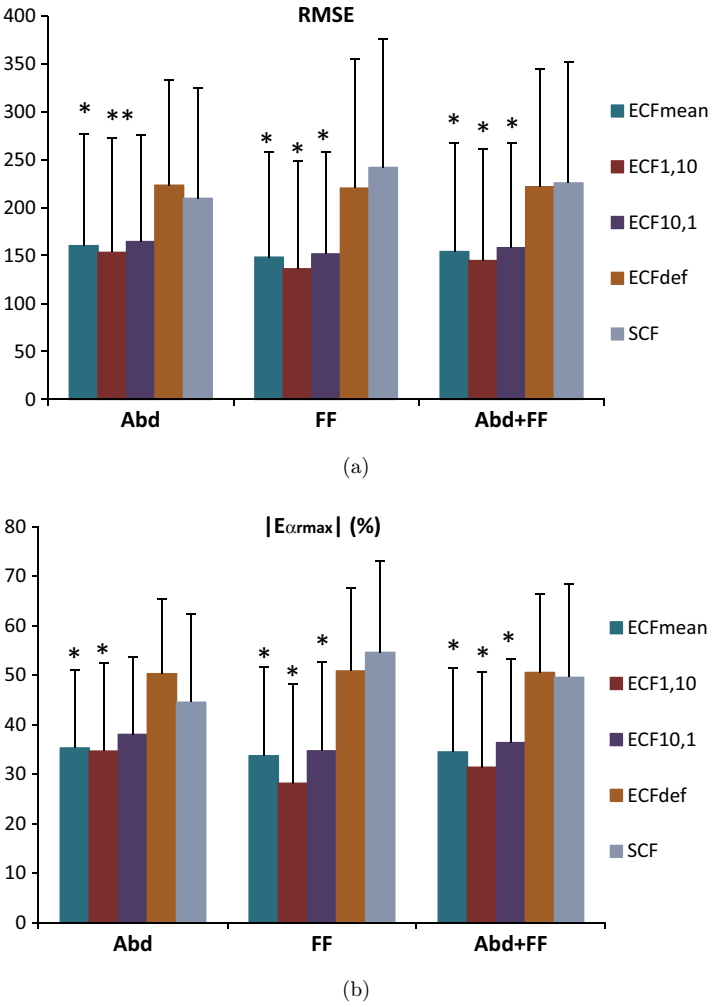

Fig. 3. The (a) RMSE and (b) absolute $E_{\alpha\,\max}$ calculated for selected combinations of the weight factors of the ECF (ECF_{mean}, $ECF_{1,10}$, and $ECF_{10,1}$), the default form of the ECF (ECF_{def}) and the SCF averaged across all measured subjects during performing Abd, FF, and both Abd + FF motions.

*Significantly different from either ECF_{def} or SCF ($p < 0.05$).

2.7. *Relative contribution of two energy terms*

Having values for wf_1 and wf_2, the relative contribution of the two energy terms (E_{cb}/E_{ca}) was calculated for different muscle elements at the maximal arm elevation angle (α_{max}) for each motion. For each subject, motion, and force ratio (i.e., F/F_{max}, Eq. (2)), the calculated E_{cb}/E_{ca} was averaged over a selection of muscle elements (i.e., muscles passing the glenohumeral joint) and averaged across all subjects and motions (Fig. 4).

J. Mech. Med. Biol. 2013.13. Downloaded from www.worldscientific.com
by VU UNIVERSITY AMSTERDAM LIBRARY on 03/25/13. For personal use only.

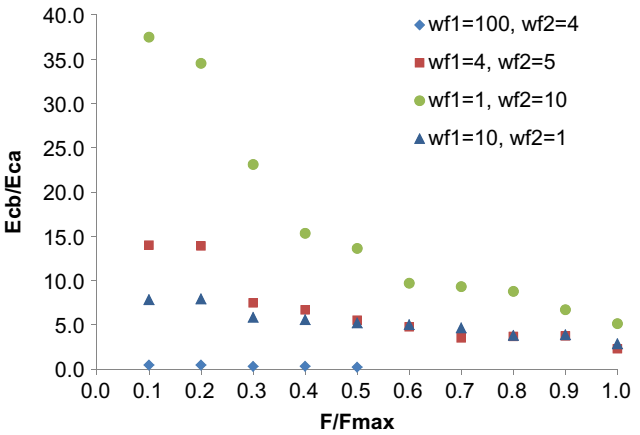

(a)

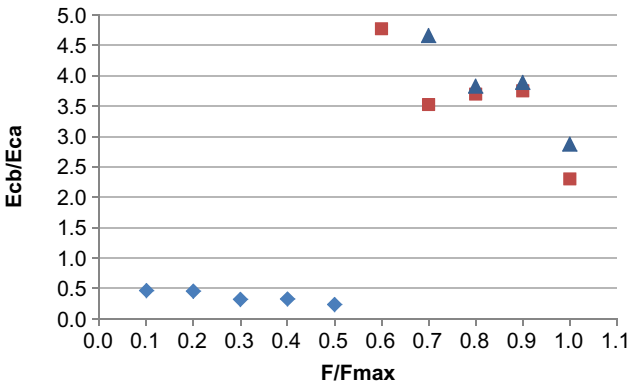

(b)

Fig. 4. (a) The relative contribution (E_{cb}/E_{ca}) of the different energy terms in the ECF *vs.* force ratio ($F/F_{\max}$, Eq. (2)), for different sets of weight factors averaged across selected muscles and all subjects. (b) Zoom in of area in part-a in which $E_{cb}/E_{ca} \leq 5$.

3. Results

3.1. *GH-JRFs*

The generic model generally underestimated the GH-JRFs when compared to the *in vivo* recordings ($E_{\alpha\,\max}$, Figs. 1–3). The results (Figs. 1 and 2) revealed that when the two weight factors simultaneously decreased, the magnitude of the RMSE and $|E_{\alpha\,\max}|$ decreased, indicating that the model estimations got closer to the measured data.

The highest deviations of the model calculations from the measurements occurred around the zone in which $10 \leq wf_1 \leq 80$ and $wf_2 = 20$ (Figs. 1 and 2).

By increasing wf_2 from 20 to 100 (giving a higher share to the nonlinear part of the calcium pumping term), the RMSE and $|E_{\alpha\,\max}|$ increased (on average ~12 % for

$|E_{\alpha\,\max}|$) for $wf_1 \leq 30$ but slightly decreased (on average $\sim 3\%$ for $|E_{\alpha\,\max}|$) for higher values of wf_1.

By using the three selected sets of weight factors for the ECF (i.e., ECF_{mean}, $\text{ECF}_{1,10}$, and $\text{ECF}_{10,1}$), the model predictions of the GH-JRFs significantly ($p < 0.05$, post-hoc power ~ 0.3) improved (on average $\sim 20\%$ at $\alpha_{\max}$) in most cases compared to when using either the ECF_{def} or the SCF (Fig. 3).

3.2. *Relative contribution of the two energy terms*

Regarding the relative contribution of different terms in the energy cost function (Fig. 4), using the selected sets of weight factors led to $E_{cb} : E_{ca}$ equal to, respectively, 2.3:1, 5.1:1, and 2.9:1 for ECF_{mean}, $\text{ECF}_{1,10}$, and $\text{ECF}_{10,1}$ at 100% muscle activation (i.e., when $F/F_{\max} = 1$). This implies that at maximal muscle activation, respectively, about 30%, 16%, and 25% of the total energy consumption is related to calcium pumping when using ECF_{mean}, $\text{ECF}_{1,10}$, and $\text{ECF}_{10,1}$.

4. Discussion

The *in vivo*-measured GH-JRFs by instrumented shoulder endoprostheses were used to identify the weight parameters of a previously developed energy-based muscle load sharing cost function. The new identified weight parameters were different from those that were originally used. By applying the new parameter sets, the model could calculate the GH-JRFs significantly closer (on average 20%) to *in vivo* measurements.

Similar to the results of our previous study,[13] not only the generic model generally underestimated the GH-JRFs compared to the *in vivo* measurements, but the predicted GH-JRFs were not identical for the default form of the energy cost function (ECF_{def}) and the stress criterion (SCF). When using the ECF_{def}, the model predicted GH-JRFs were slightly lower ($\sim 6\%$) during Abd motion, but not notably higher ($\sim 4\%$) during FF motion.

Using all selected parameter sets for ECF (i.e., ECF_{mean}, $\text{ECF}_{1,10}$, and $\text{ECF}_{10,1}$) resulted in significant improvements in the modeling calculations; one would expect a final recommended parameter set for future applications. The cost function with this selected parameter set not only should have the capability of considerably improving the model predictions, but also should lead to a relative contribution of the energy terms, which is in agreement with the corresponding values in the literature. Among the selected solutions, the $\text{ECF}_{1,10}$ had the lowest average values of both RMSE and $|E_{\alpha\,\max}|$ (Fig. 3). However, when using the $\text{ECF}_{1,10}$, the relative contributions of the energy terms at lower muscle activations (i.e., $F/F_{\max} < 0.3$) do not seem feasible. Moreover, the contribution of the calcium pumping at maximal activation [$\sim 16\%$, Fig. 4(a)] does not coincide with reported values for single muscles that range from 23% to 44%.[15–21,27] The other two parameter sets (ECF_{mean} and $\text{ECF}_{10,1}$) resulted in contributions for calcium pumping (30% and 25%) that were more similar to the range of these reported values. Although ECF_{mean} gave slightly better results ($\sim 3\%$)

J. Mech. Med. Biol. 2013.13. Downloaded from www.worldscientific.com
by VU UNIVERSITY AMSTERDAM LIBRARY on 03/25/13. For personal use only.

than the $ECF_{10,1}$ (Fig. 3), $ECF_{10,1}$ showed a smoother pattern of the $E_{cb} : E_{ca}$ at different muscle activations (Fig. 4). We therefore recommend the $ECF_{10,1}$ as the new selected parameter set for the ECF for modeling standard tasks like Abd and FF.

The increase in the magnitude of the model-predicted GH-JRFs when using the new parameter sets compared to the default form of the ECF and/or the SCF is related to the increase in model-predicted individual muscle forces (Fig. 5). For Abd, using the new identified parameter set mostly affected the model prediction of the trapezius scapular part, serratus anterior, supraspinatus, biceps (long and/or short heads), and triceps medialis muscle forces. During FF motion, the model prediction

J. Mech. Med. Biol. 2013.13. Downloaded from www.worldscientific.com
by VU UNIVERSITY AMSTERDAM LIBRARY on 03/25/13. For personal use only.

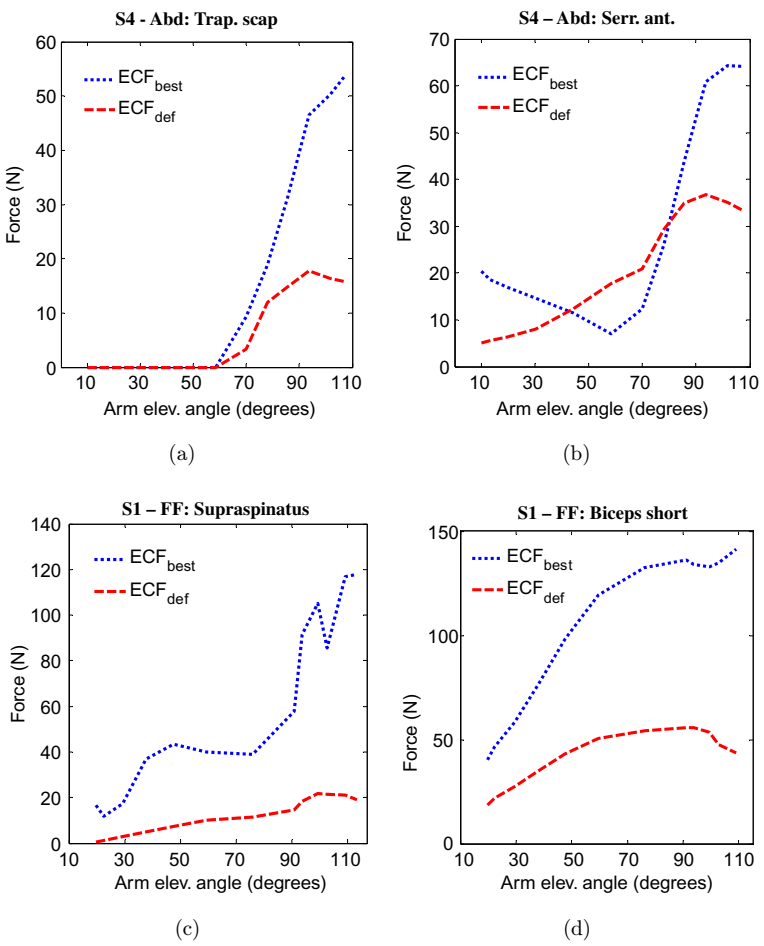

Fig. 5. Comparing the model-estimated muscle forces using the best solution and the default set for the ECF *vs.* arm elevation angle for subjects who could elevate their arm at angles above 90°.

Abd: abduction; FF: forward flexion; Trap. scap.: Trapezius scapular part muscle, Serr. ant.: Serratus anterior muscle.

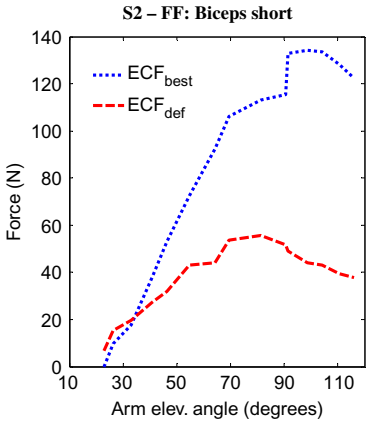

(e)

Fig. 5. (*Continued*)

of the serratus anterior, supraspinatus, biceps short head, and triceps medialis muscle forces considerably increased when using the new identified parameter set.

As results showed (Figs. 1 and 2), by either directly (wf_1) or indirectly (wf_2) decreasing the contribution of the calcium pumping with respect to the detachment of cross-bridges in the energy cost function, the model-predicted GH-JRFs increased. The role of wf_2 (i.e., a nonlinear quadratic term in the calcium pumping part) is more prominently highlighted at the lower values of wf_1 (< 70). Praagman *et al.*[9,10] found less false-negatives for model-estimated forces to EMG comparisons when using a nonlinear quadratic term in the calcium pumping part, however, there is no (quantitative) proof about whether or not considering this nonlinear term leads to improvements in the model predictions. It has been stated that the linear muscle load sharing criteria generally favor discrete muscle action, while the nonlinear criteria basically lead to synergism.[8,35] Nevertheless, considering that by increasing the share of the nonlinear term in the energy cost function decrease the model-predicted GH-JRFs, it seems that this nonlinear term does not play a major role in changing the synergism of muscle force sharing.

A generic inverse dynamics model was used for modeling purposes in this study. The morphological differences between the cadaver from which the model parameters have been obtained and measured subjects could be a potential source of differences between the model and experiments (i.e., the general GH-JRFs underestimation). The large interindividual variability in both the bony and muscular anatomy can change many parameters such as the position of the joint rotation centers, moment arms, and muscle strength parameters (e.g., PCSA and volume). Moreover, replacing the physiological processes and/or complex anatomical structures by mechanical constraints and/or simplified geometrical shapes in the model may have caused inconsistencies between the model and experiments. However, to

J. Mech. Med. Biol. 2013.13. Downloaded from www.worldscientific.com
by VU UNIVERSITY AMSTERDAM LIBRARY on 03/25/13. For personal use only.

J. Mech. Med. Biol. 2013.13. Downloaded from www.worldscientific.com
by VU UNIVERSITY AMSTERDAM LIBRARY on 03/25/13. For personal use only.

what extent such model simplifications or morphological differences can affect the modeling results is not a clear issue. Subject-specific modeling[36,37] is the most recent technique which can be applied to quantify the effects of geometrical simplifications.

Other than the general underestimation of the model, the estimated and measured GH-JRFs also behaved differently at arm elevation angles above 90° (increasing measured *vs.* decreasing model-estimated). As previously proposed[13] the different behaviors can be caused by muscle co-contraction based on either a standard or pathological (related to endoprosthesis) coordination pattern. Researchers have developed and used advanced muscle load sharing cost functions in order to consider the muscle co-contraction in the modeling procedure.[38,39] Among the four measured subjects in the current study, two subjects (S2 and S4) were able to elevate their arms above 90° during both Abd and FF, while subject S1 could only do so during flexion motion. Using the new identified parameters in the current study demonstrated the potential to improve the pattern of the model-predicted GH-JRFs for above 90° in three cases (Fig. 6). Nevertheless, this effect seems to be fairly random considering that the tuned criterion did not have any effect on the pattern of the model-predicted GH-JRFs above 90° for S2 during Abd (Fig. 6(a)) and S4 during FF (Fig. 6(e)).

EMG-driven modeling is an alternative approach to account for possible antagonist co-contraction. The results of our recent study[40] revealed that including the EMGs as input to the model could considerably improve (up to 45%) the model predictions of the GH-JRFs, especially for angles above 90°. ECF_{def} was used as the muscle load sharing criterion in that study. One should, however, note that the mechanisms that improve the pattern of the model-predicted GH-JRFs at angles

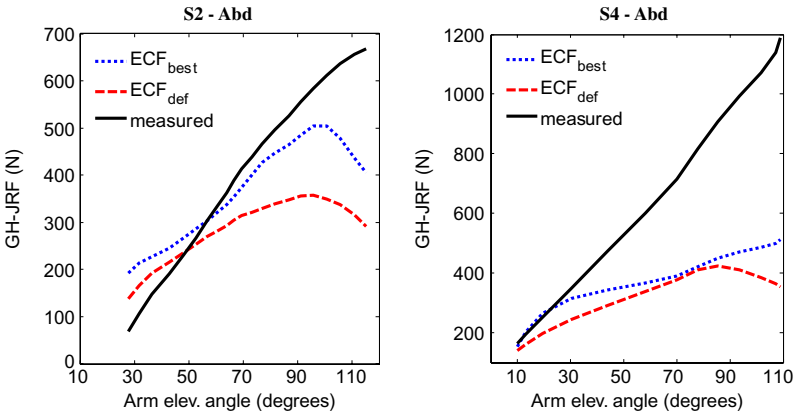

(a) (b)

Fig. 6. Comparing the model-estimated using the best solution (ECF_{best}, Table 3) and the default set (ECF_{def}) for the ECF and the measured GH-JRFs *vs.* arm elevation angle for subjects who could elevate their arm at angles above 90°.

Abd: abduction; FF: forward flexion.

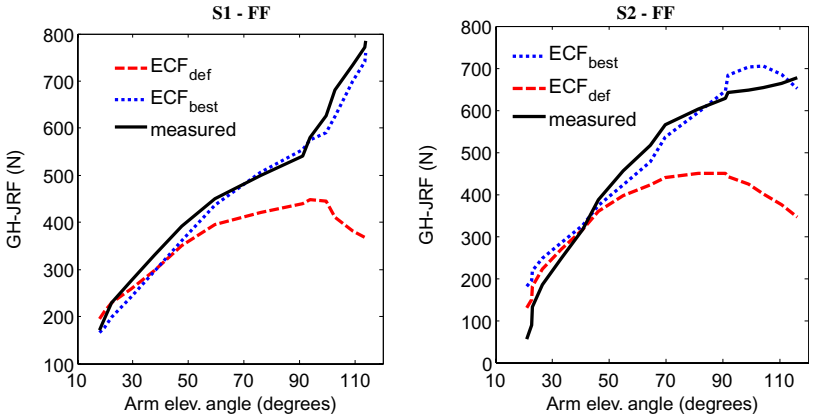

(c) (d)

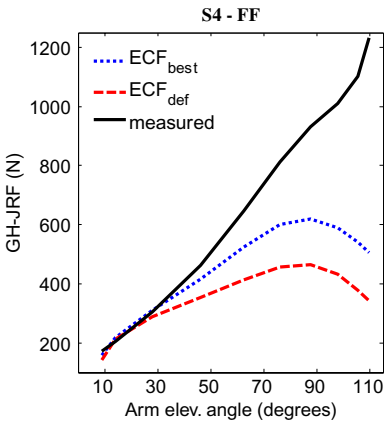

(e)

Fig. 6. (*Continued*)

above 90° were not identical in the two approaches. In the EMG-driven model, the force behavior above 90° was improved by forcing the model to mimic the recorded activation pattern of the major antagonist co-contractors such as the pectoralis major clavicular (during Abd) or deltoid posterior part (during FF). The tuned parameter set for the ECF (ECF_{best}) affected the model predictions of the GH-JRFs by giving an incremental load share for angles above 90° to muscles like the trapezius scapular part, serratus anterior, supraspinatus, and/or biceps short (Fig. 5).

Other than the energy processes presented in the current energy-based criterion, there are also several energy processes that have not been accounted for. Previously, the sodium ion (Na^+-K^+) turnover was not thought to have a contribution in total energy turnover. However, some recent studies[27,41] showed that during the first few seconds of stimulation, about 5−10% of the total energy turnover can relate to Na^+-K^+

J. Mech. Med. Biol. 2013.13. Downloaded from www.worldscientific.com
by VU UNIVERSITY AMSTERDAM LIBRARY on 03/25/13. For personal use only.

pumping, indicating that Na^+-K^+ pumping could potentially have some impact on the energy consumption of the skeletal muscle. Therefore, for the construction of a more physiologically-oriented criterion, one needs to consider Na^+-K^+ pumping as a separate energy process in the energy-based muscle load sharing cost function.

Another important aspect is the higher energy rate associated with shortening, sometimes called the Fenn effect.[42,43] Neglecting the Fenn effect may limit the implementation of the ECF in high-speed dynamic movements. Given that some muscles shorten at different rates during fast dynamic movements, it is likely to have an impact on the estimates of energy cost. Thus, for the application of the ECF in fast dynamic movements (e.g., throwing ball in baseball), the Fenn effect should also be taken into account.

J. Mech. Med. Biol. 2013.13. Downloaded from www.worldscientific.com
by VU UNIVERSITY AMSTERDAM LIBRARY on 03/25/13. For personal use only.

5. Conclusions

The relative contribution of two muscle energy consumption processes including the detachment of cross-bridges and the calcium pumping incorporating in the energy-based criterion was quantified by using *in vivo*-measured GH-JRFs on four patients carrying an instrumented shoulder implant. A set of new weight parameters which determined the relative contribution of the energy term was identified. The energy-based criterion with the new identified parameter set resulted not only in significant improvements of the model calculated GH-JRFs, but also a relative contribution of the two energy terms at maximal muscle activation, coinciding with the corresponding values in the literature for isometric contraction. The new identified parameter set is therefore recommended to be used instead of previously used parameters.

References

1. Nikooyan AA, Zadpoor AA, Mass-spring-damper modeling of the human body to study running and hopping: An overview, *P I Mech Eng H* **225**:1121−1135, 2011.
2. Nikooyan AA, Zadpoor AA, An improved cost function for modeling of muscle activity during running, *J Biomech* **44**:984−987, 2011.
3. Nikooyan AA, Zadpoor AA, Effects of muscle fatigue on the ground reaction force and soft tissue vibrations during running: A model study, *IEEE Trans Biomed Eng* **59**:797−804, 2012.
4. Berthonnaud E, Morrow M, Herzberg G, An KN, Dimnet J, Biomechanical model predicting values of muscle forces in the shoulder girdle during arm elevation, *J Mech Med Biol* **10**:643−666, 2010.
5. Erdemir A, McLean S, Herzog W, van den Bogert AJ, Model-based estimation of muscle forces exerted during movements, *Clin Biomech* **22**:131−154, 2007.
6. Rupp TK, Schmitt S, Inverse dynamics of the lower extremities: Novel approach considering talocrural and subtalar joint axis, *J Mech Med Biol* **11**:515−527, 2011.
7. Tsirakos D, Baltzopoulos V, Bartlett R, Inverse optimization: Functional and physiological considerations related to the force-sharing problem, *Crit Rev Biomed Eng* **25**:371−407, 1997.

J. Mech. Med. Biol. 2013.13. Downloaded from www.worldscientific.com
by VU UNIVERSITY AMSTERDAM LIBRARY on 03/25/13. For personal use only.

8. Crowninshield RD, Brand RA, A physiologically based criterion of muscle force prediction in locomotion, *J Biomech* **14**:793−801, 1981.
9. Praagman M, Muscle load sharing: An energy-based approach, Ph. D. Thesis, VU University Amsterdam, 2008.
10. Praagman M, Chadwick EKJ, van der Helm FCT, Veeger HEJ, The relationship between two different mechanical cost functions and muscle oxygen consumption, *J Biomech* **39**:758−765, 2006.
11. Nikooyan AA, Veeger HEJ, Chadwick EKJ, Praagman M, van der Helm FCT, Development of a comprehensive musculoskeletal model of the shoulder and elbow, *Med Biol Eng Comput* **49**:1425−1435, 2011.
12. Steenbrink F *et al.*, Arm load magnitude affects selective shoulder muscle activation, *Med Biol Eng Comput* **47**:565−572, 2009.
13. Nikooyan AA *et al.*, Validation of the Delft Shoulder and Elbow Model using *in vivo* glenohumeral joint contact forces, *J Biomech* **43**:3007−3014, 2010.
14. Westerhoff P, Graichen F, Bender A, Rohlmann A, Bergmann G, An instrumented implant for *in vivo* measurement of contact forces and contact moments in the shoulder joint, *Med Eng Phys* **31**:207−213, 2009.
15. Barclay CJ, Constable JK, Gibbs CL, Energetics of fast-twitch and slow-twich muscles of the mouse, *J Physiol* **472**:61−80, 1993.
16. Barclay CJ, Lichtwark GA, Curtin NA, The energetic cost of activation in mouse fast-twitch muscle is the same whether measured using reduced filament overlap or N-benzyl-p-toluenesulphonamide, *Acta Physiol* **193**:381−391, 2008.
17. Homsher E, Mommaerts WFHM, Ricchiuti NV, Wallner A, Activation heat, activation metabolism and tension-related heat in frog semitendinosus muscles, *J Physiol* **220**:601−625, 1972.
18. Rome LC, Klimov AA, Superfast contractions without superfast energetics: ATP usage by SR-Ca2+ pumps and crossbridges in toadfish swimbladder muscle, *J Physiol* **526**:279−286, 2000.
19. Stienen GJM, Zaremba R, Elzinga G, ATP utilization for calcium uptake and force production in skinned muscle fibres of *Xenopus laevis*, *J Physiol* **482**:109−122, 1995.
20. Szentesi P, Zaremba R, van Mechelen W, Stienen GJM, ATP utilization for calcium uptake and force production in different types of human skeletal muscle fibres, *J Physiol* **531**:393−403, 2001.
21. Walsh B, Howlett RA, Stary CM, Kindig CA, Hogan MC, Measurement of activation energy and oxidative phosphorylation onset kinetics in isolated muscle fibers in the absence of cross-bridge cycling, *A J Physiol Reg I* **290**:R1707−R1713, 2006.
22. Burchfield DM, Rall JA, Energetics of activation in frog skeletal muscle at sarcomere lengths beyond myofilament overlap, *Biophys J* **48**:1049−1051, 1985.
23. Rall JA, Effects of temperature on tension, tension-dependent heat, and activation heat in twitches of frog skeletal muscle, *J Physiol* **291**:265−275, 1979.
24. Rall JA, Schottelius BA, Energetics of contraction in phasic and tonic skeletal muscles of the chicken, *J Gen Physiol* **62**:303−323, 1973.
25. Wendt IR, Barclay JK, Effects of dantrolene on the energetics of fast- and slow-twitch muscles of the mouse, *Am J Physiol* **238**:C56−C61, 1980.
26. Zhang SJ, Andersson DC, Sandstrom ME, Westerblad H, Katz A, Cross bridges account for only 20% of total ATP consumption during submaximal isometric contraction in mouse fast-twitch skeletal muscle, *Am J Physiol-Cell Ph* **291**:C147−C154, 2006.
27. Barclay C, Woledge R, Curtin N, Energy turnover for Ca^{2+} cycling in skeletal muscle, *J Muscle Res Cell Mutil* **28**:259−274, 2007.

28. Van der Helm FCT, A finite element musculoskeletal model of the shoulder mechanism, *J Biomech* **27**:551−553, 1994.
29. Klein Breteler MD, Spoor CW, Van der Helm FCT, Measuring muscle and joint geometry parameters of a shoulder for modeling purposes, *J Biomech* **32**:1191−1197, 1999.
30. An KN, Kaufman KR, Chao EYS, Physiological considerations of muscle force through the elbow joint, *J Biomech* **22**:1249−1256, 1989.
31. Winters JM, Stark L, Analysis of fundamental human movement patterns through the use of in-depth antagonistic muscle models, *IEEE Trans Biomed Eng* **32**:826−839, 1985.
32. Wu G *et al.*, ISB recommendation on definitions of joint coordinate systems of various joints for the reporting of human joint motion−Part II: Shoulder, elbow, wrist and hand, *J Biomech* **38**:981−992, 2005.
33. Nikooyan AA *et al.*, Comparison of two methods for *in vivo* estimation of the gleno-humeral joint rotation center of the patients with shoulder hemiarthroplasty, *PLoS One* **6**:e18488, 2011, from http://www.plosone.org/article/info%3Adoi%2F10.1371%2Fjournal.pone.0018488.
34. Karduna AR, McClure PW, Michener LA, Sennett B, Dynamic measurements of three-dimensional scapular kinematics: A validation study, *J Biomech Eng* **123**:184−190, 2001.
35. Dul J, Townsend MA, Shiavi R, Johnson GE, Muscular synergism-I. On criteria for load sharing between synergistic muscles, *J Biomech* **17**:663−673, 1984.
36. Baudoin A, Skalli W, de Guise J, Mitton D, Parametric subject-specific model for *in vivo* 3D reconstruction using bi-planar X-rays: Application to the upper femoral extremity, *Med Biol Eng Comput* **46**:799−805, 2008.
37. Berthonnaud E, Fougier P, Hilmi R, Labelle H, Dimnet J, Relationship between sagittal spinal curves and back surface profiles obtained with radiographs, *J Mech Med Biol* **10**:313−325, 2010.
38. Forster E, Simon U, Augat P, Claes L, Extension of a state-of-the-art optimization criterion to predict co-contraction, *J Biomech* **37**:577−581, 2004.
39. Jinha A, Ait-Haddou R, Herzog W, Predictions of co-contraction depend critically on degrees-of-freedom in the musculoskeletal model, *J Biomech* **39**:1145−1152, 2006.
40. Nikooyan AA *et al.*, An EMG-driven musculoskeletal model of the shoulder, *Hum Mov Sci* **31**:429−447, 2012.
41. Clausen T, Na^+-K^+ pump regulation and skeletal muscle contractility, *Physiol Rev* **83**:1269, 2003.
42. Alexander RM, Optimum muscle design for oscillatory movements, *J Theory Biol* **184**:253−259, 1997.
43. Lichtwark GA, Wilson AM, A modified Hill muscle model that predicts muscle power output and efficiency during sinusoidal length changes, *J Exp Biol* **208**:2831−2843, 2005.

J. Mech. Med. Biol. 2013.13. Downloaded from www.worldscientific.com
by VU UNIVERSITY AMSTERDAM LIBRARY on 03/25/13. For personal use only.